Advances in Industrial and Manufacturing Engineering 10 (2025) 100156

Contents lists available at ScienceDirect

Advances in Industrial and Manufacturing Engineering

journal homepage: www.sciencedirect.com/journal/advances-in-industrial-and-manufacturing-engineering

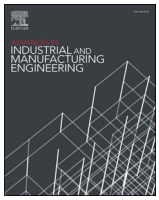

Analytical criterion to prevent thermal overshoot during dynamic curing of thick composite laminates

Jordi Farjas [b], José Antonio González [a], Daniel Sánchez-Rodríguez [b,*], Norbert Blanco [a], Marc Gascons [a], Josep Costa [a]

[a] AMADE - Analysis and Advanced Materials for Structural Design, Polytechnic School, University of Girona, C/ Universitat de Girona 4, E-17003, Girona, Spain
[b] GRMT Materials Research Group and Thermodynamics, Polytechnic School, University of Girona, C/ Universitat de Girona 4, E-17003, Girona, Spain

ARTICLE INFO

Keywords:
Laminates
Cure behaviour
Process modeling
Autoclave

ABSTRACT

Local overheating during curing of thermosetting resins is likely to occur for thick laminates or during fast curing. Overheating may lead to heterogeneous mechanical properties along the laminate thickness or even to an uncontrolled reaction. To avoid overheating, most thermoset resin manufacturers recommend a "safe" cure cycle. However, these cure cycles can be improved to shorten cure times in thin laminates and may not be good enough to avoid overheating in thick laminates. In this paper, we propose a new analytical model to determine the critical thickness above which thermal runaway occurs when the laminate is heated at a constant rate up to a constant temperature. The model considers different thermal boundaries between the mould and the laminate, i.e., from a perfect thermal contact to a contact of infinite resistance. The analytical model was corroborated through the numerical integration of the equations governing it and experimental data from the curing process of a thick laminate composed of the commercial VTC401 epoxy resin and M55J carbon fiber system. Model predictions indicate that, under the manufacturer's recommended cure cycle, which includes an initial heating rate of 2 K/min, thermal runaway occurs in laminates thicker than 12.4 mm, aligning with experimental observations. A 20-mm-thick laminate, exceeding this threshold, was cured using a reduced heating rate of 0.3 K/min based on our criteria, successfully preventing overheating. The maximum temperature gradient recorded experimentally remained below 1 °C, confirming the model's prediction of uniform thermalization.

1. Introduction

The main problem of fast curing and curing of thick carbon-epoxy laminates lies in the removal of the heat generated by the exothermic reaction (Lorenz et al., 2022). Due to the low thermal conductivity of the thermoset, in fast cure cycles and thick samples, the heat released by the curing process is not dissipated effectively, the local temperature rises, and the rate of reaction and heat generation increases. The formation of temperature gradients leads to non-uniform curing, morphological inhomogeneities, and even the degradation of the matrix and delamination (Ciriscioli et al., 1992; Twardowski et al., 1993). For example, these issues are commonly found in rapid autoclave curing, which often presents an unacceptable risk of exothermic overshoots (Tifkitsis et al., 2018; Voto et al., 2019). Eventually, when the sample exceeds a critical condition, this enhancement of the reaction rate induces a thermal runaway (Barzykin, 1973; Merzhanov and Strunina, 1965).

The occurrence of a thermal runaway depends on two time scales: the reaction time, and the heat dissipation time. Therefore, a thermal runaway occurs when the dissipation time is longer than the reaction time (Adler and Enig, 1964; Varma et al., 1999). Fast curing implies a reduction in the reaction time, while the dissipation time increases in thick laminates. Therefore, in both cases, this favours the occurrence of a thermal runaway, meaning that the generation and transfer of heat must be considered to predict the result of a cure cycle in fast curing conditions and in thick composite parts (Zhang et al., 2021). For instance, the manufacturer's recommended cure cycle (MRCC), commonly used for thin laminates, may not be valid for thick composite parts. In this case, the occurrence of a thermal runaway is manifested by a characteristic temperature overshoot (Michaud et al., 2002; Oh and Lee, 2002). As a result, conservative long curing cycles are adopted for thick parts, with the consequent penalty in manufacturing costs. Therefore, to optimise the cure cycle, tools are needed to determine the conditions under which a sample will experience a thermal runaway.

So far, several numerical methods have been developed to analyse

* Corresponding author.
E-mail address: daniel.sanchez@udg.edu (D. Sánchez-Rodríguez).

https://doi.org/10.1016/j.aime.2024.100156
Received 1 August 2024; Received in revised form 20 December 2024; Accepted 23 December 2024
Available online 24 December 2024

overheating during the curing process of fibre reinforced polymer (FRP) laminates (Bogetti and Gillespie, 1991; Dolkun et al., 2018). Voto et al. (2019) developed a one-dimensional (1D) model of the heat flow balance to determine the heating rate limit in fast cure processing of thick laminates. Tifkitsis et al. (2018) developed a stochastic multi-objective methodology for optimizing the curing of thick epoxy/carbon fibre laminates. They used a surrogate model embedded in a genetic algorithm-based framework. Their two-dimensional (2D) model includes insulating and convective boundaries. Esposito et al. (2016) presented a 2D finite element model that introduces the heat flow produced by convection inside the autoclave and conduction between the aluminium mould and the laminate. The model takes into account the breather material. Shi (Shi, 2016) followed a similar approach, but the application was carried out using a three-dimensional (3D) heat transfer model. The overheating predictions for a 32-mm-thick flat panel showed almost the same accuracy as the 2D model. Sorrentino et al. (2017) evaluated the effect of curing overheating on mechanical properties (ILSS). Their results revealed that, an exothermic peak of 52 °C (17-mm-thick carbon-epoxy panels) above the dwell temperature causes a decrease in interlaminar shear strength of 8.3 %, while a peak of 75 °C (25 mm thick) results in a reduction of ILSS of 17.1 %. The overheating predictions for a 32-mm-thick flat panel showed practically the same accuracy as the 2D model.

While integrating numerical models is certainly an advance over trial-and-error procedures for optimizing curing cycles, implementing them within an industrial context is still challenging. In the one hand, the iterative nature of running multiple simulations to achieve the optimal cure cycle can be very time-consuming and computationally demanding. Besides, the implementation of the solving algorithms typically relies on commercial software packages. These packages often require extensive numerical procedures and specialized personnel to manage them. Moreover, commercial simulation software usually involves high licensing costs. As an alternative to simulations, attempts have been made to establish a framework for guiding the processing of thick laminate based on studying the sensitivity of various curing parameters to specimen thickness (Gao et al., 2023). However, the conclusions drawn from such studies tend to be merely qualitative. On the other hand, obtaining an analytical solution to the thermal overshoot problem would significantly enhance rapid decision-making when optimizing curing cycles for thick laminates. Such a solution would indeed elucidate the dependencies of system parameters, providing direct insight into how process variables influence system behaviour. Furthermore, once derived, these solutions are straightforward and quick to compute.

However, to the best of our knowledge, there are no analytical models available to predict the occurrence of thermal runaways in composites processed under constant heating rates. This work introduces a criterion, based on an analytical model, designed to prevent thermal runaway during the processing of thermoset laminates under constant heating rates. The criterion incorporates heat convection and is applicable to various processing techniques, such as infusion and simple bake plate curing. Specifically, we adapt and expand the thermal runaway criterion developed by Sánchez-Rodríguez et al. (Sánchez-Rodriguez et al., 2017a, 2017b) to account for the typical curing process conditions of hot plate pressing and vacuum infusion manufacturing, which has not been previously addressed. We consider the case of constant heating, and the analytical criterion is validated by comparing it with the numerical integration of the corresponding partial differential equation. As a further validation case, we study experimentally the thermal evolution during curing according to the MRCC of a 20-mm-thick laminate made of VTC401/M55J.

2. Materials and experimental methods

The composite laminate used in this study was manufactured using M55J/VTC401 carbon epoxy unidirectional prepreg (SHD Composite Materials Ltd). It has an aerial weight of 100 g/m^2 and 32% resin content in weight (VTC401 *Epoxy Component Press et al., 1994*). Thermal, kinetic, and physical properties are reported in Table 1.

Two flat 300 × 300 × 20 mm^3 panels were laminated by prepreg hand lay-up and subsequently cured into a conventional autoclave system. An aluminium mould was cleaned and covered with polyolefin non-perforated release film. The prepreg layers were cut to size and placed on the mould until the $[0^\circ]_{200}$ laminate stacking sequence was completed. A standard peel-ply was placed on top of the laminate. A Teflon coated glass fabric was used as an edge breather to remove entrapped air from the laminate stack. A commercial non-woven polyester breather (330 g/m^2) was used for an even distribution of vacuum. The entire setup was sealed using a vacuum bag with bagging tape, while the vacuum pressure was 0.95 bar. During the lamination process, debulking was performed after the first layer and then every three layers after that, by applying the vacuum for 5 min to remove the entrapped air from the laminate stack and ensure good prepreg compaction. Fig. 1 details the bagging scheme. One of the panels was subjected to the MRCC (see section 5), while the second one was subjected to a modified cycle based on the analytical model and designed to avoid the formation of thermal gradients.

Six thermocouples were embedded through the panel thickness (Fig. 2), and the autoclave temperature was controlled by the coldest of the thermocouples embedded in the CFRP panel.

For the panel submitted to the MRCC, a slice was cut from the centre of the panel using a diamond saw and two 10 × 5 × 3 mm^3 samples were extracted from the inside of the CFRP panel (indicated in blue in Fig. 3) and from the area adjacent to the tool (in green) to study the variation of the glass transition temperature (T_g) across the thickness (Fig. 3).

The T_g was obtained using a DSC from TA Instruments, Model Q2000. The temperature range was 30 °C to 250 °C at a heating rate of 10 °C/min. Aluminium pans were used for the reference and the samples. Measurements were taken with a continuous purge of nitrogen (99.999 % purity) at a flow rate of 50 ml/min.

3. Thermochemical model

For large surface area parts, the temperature gradients normal to z-axis (see Fig. 4) are negligible. Under this assumption, the thermal problem can be reduced to the balance between the heat generated locally by the curing reaction and the heat propagation through the sample:

$$\rho c \frac{\partial T}{\partial t} = \kappa \frac{\partial^2 T}{\partial z^2} + \rho q \frac{\partial \alpha}{\partial t}, \tag{1}$$

where T is the temperature, t is the time, z is the space coordinate (see Fig. 4), ρ is the density, c is the specific heat capacity, κ is the thermal conductivity, q is the enthalpy of the reaction, and $\alpha(z,t)$ is the degree of cure ($\alpha = 0$ untransformed, $\alpha = 1$ totally cured). We assume that the physical parameters are independent of the temperature and degree of cure.

As for the reaction, we assume a first-order reaction kinetics to account for the reactant consumption. While this approach simplifies the actual evolution of the reaction kinetics, it has proven to be a reasonable

Table 1
Physical and kinetic properties of the M55J/VTC401 UD prepreg (*Approximated value, taken from carbon-epoxy UD M21/T700).

Thermal conductivity out-of-plane, κ (W m^{-1} K^{-1}) (Tranchard et al., 2017)	0.85*
Specific heat capacity, c (J kg^{-1} K^{-1}) (Tranchard et al., 2017)	1150*
Density, ρ (kg m^{-3})	1686
Specific heat of reaction, q (J kg^{-1}) (González Ruiz et al., 2022)	2.1 × 10^5
Activation energy, E_A (J mol^{-1}) (González Ruiz et al., 2022)	9.17 × 10^4
Pre-exponential constant, A (s^{-1}) (González Ruiz et al., 2022)	3.0 × 10^9

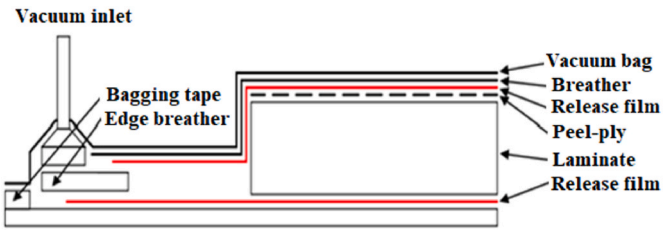

Fig. 1. Vacuum bagging scheme of the manufactured panel.

approximation for predicting the onset of thermal runaway, particularly when it occurs in the early stages of the reaction, as demonstrated in studies on metallorganic precursors (Sánchez-Rodríguez et al., 2017) and propellants (Victor, 1995). Moreover, the reaction is assumed to be thermally activated following an Arrhenius temperature dependence, i.e.:

$$\frac{\partial \alpha}{\partial t} = A e^{-E_A/R_G T}(1-\alpha) \tag{2}$$

where A is the pre-exponential factor, E_A is the activation energy, and R_G is the universal gas constant (8.314 J K^{-1}·mol^{-1}).

Initially, we assume that the initial sample temperature, T_{in}, is uniform and equal to 293 K (room temperature), and that the degree of transformation is zero throughout the sample. We assume that heat transfer through the top surface of the laminate is controlled by gas convection, and that the gas temperature corresponds to that of the mould, T_m. As for the bottom surface, we assume that there is a perfect thermal contact with the mould and that its temperature is T_m:

$$\kappa \left.\frac{\partial T}{\partial z}\right|_{z=H} = h[T_m - T(H)], \kappa \left.\frac{\partial T}{\partial z}\right|_{z=0} = \kappa_m \left.\frac{\partial T}{\partial z}\right|_{z=0}, T(-H_m) = T_m \tag{3}$$

where h is the convective heat transfer coefficient (ranges from 30 to 100 $Wm^{-2}K^{-1}$ (Antonucci et al., 2001)), κ_m is the thermal conductivity of the mould, H is the thickness of the laminate, and H_m is the thickness of the mould (see Fig. 4).

To numerically solve the partial differential equation (PDE), Eq (1), we have used a fully implicit finite differences method (Press et al., 1994). Implicit methods are especially suited to thermal runaway problems because they have the ability to deal with very different time scales.

4. Analytical solution

In this section we determine the temperature range in which a thermal runaway occurs, as well as the critical laminate thickness, H_c, to avoid thermal runaways when the mould temperature is raised at a constant rate β:

$$T_m = T_{in} + \beta t, \tag{4}$$

where T_{in} is the initial temperature (typically room temperature).

Normally, T_{in} is low enough that the reaction rate is so slow that overheating related to the heat released by the curing reaction does not occur. Under these conditions, the hottest place is the one next to the mould (see Appendix), so we can initially consider the mould temperature to be representative of the sample:

$$\frac{d\alpha}{dt} = A e^{-E_A/R_G T_m}(1-\alpha). \tag{5}$$

Then, the transformation rate increases because the term $Ae^{-E_A/R_G T_m}$ increases as T_m rises. However, as the curing reaction progresses the

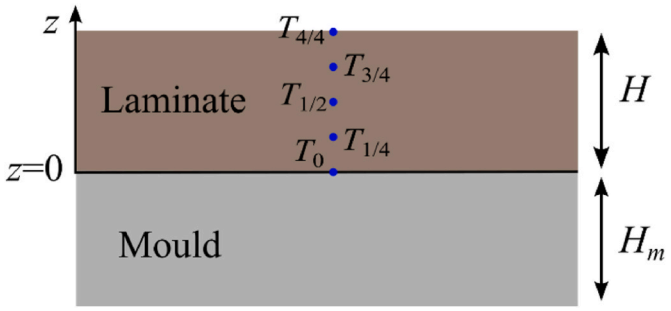

Fig. 4. Schematic representation of the geometry analysed, Eqs. (1) and (3).

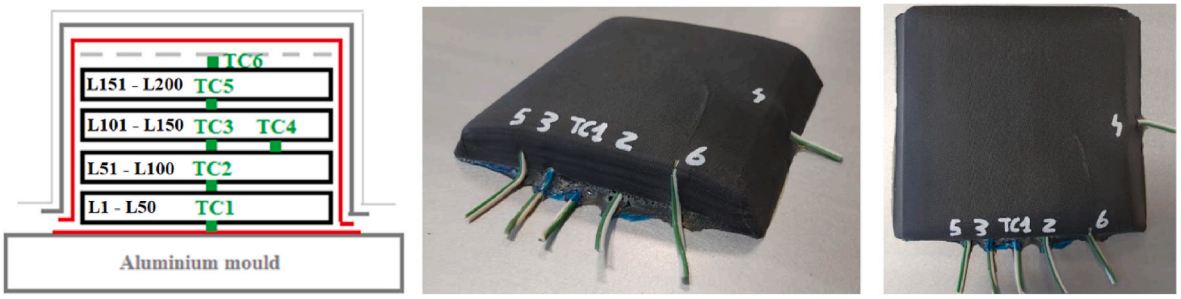

Fig. 2. Left: Schematic of the central cross-section of the panel showing the locations of the embedded thermocouple measurement junctions. (L stands for layer). Centre and Right: manufactured CFRP panel.

Fig. 3. Location of the samples extracted to determine T_g by DSC.

term $(1-\alpha)$ decreases, and the transformation rate tends to zero as the process approaches completeness. Therefore, the evolution of $d\alpha/dt$ with T_m exhibits a peaked shape and the maximum transformation rate is reached when T_m is T_{max} (see Fig. 5). The peak temperature, T_{max}, also known as Kissinger temperature, depends on β and the kinetic parameters (Farjas and Roura, 2014; Kissinger, 1957):

$$\frac{E_A}{R_G T_{max}^2} = \frac{A}{\beta} e^{-E_A/R_G T_{max}} \quad (6)$$

The thermal runaway occurs at the vicinity of the Kissinger temperature (Sánchez-Rodriguez et al., 2017b). An exact and simple approximate solution of Eq. (6) is given in references (Farjas and Roura, 2014; Roura and Farjas, 2009), respectively. Although this solution is derived from the assumption of a first order reaction model, it has been shown that the accuracy of this equation is minimally dependent on the reaction model and is primarily related to $E_A/(R_G T_{max})$ (Criado and Ortega, 1986; Šesták et al., 2014). Therefore, the validity of Eq. (5) can be considered independent of the reaction model. In particular, the percent error in the calculation of T_{max} by using this equation is negligible when $E_A/(R_G T_{max}) > 10$ (Budrugeac and Segal, 2007). For the curing of epoxy resins $E_A/(R_G T_{max}) \approx 25$ and therefore it can be applied.

Due to the heat released by the curing process, the reaction is accelerated, the duration of the curing process is reduced and therefore completed at a lower temperature, even when the critical condition for a thermal runaway has not been met (Farjas et al., 2012). To establish a limit temperature below which the reaction rate is negligible, $T_{o,r}$, we applied the method developed in (Farjas et al., 2010; Farjas and Roura, 2008) to determine the peak width at half maximum. In particular, we have obtained an approximate solution of Eq. (5):

$$\alpha(t') = 1 - exp\,[-exp\,(t'/\tau)]. \quad (7)$$

where $t' = t - \frac{T_{max} - T_{in}}{\beta}$ (that is when $t' = 0$ then $T_m = T_{max}$) and $\tau = \frac{R_G T_{max}^2}{\beta E_A}$ is a time constant. Note, that the solution of Eq. (7) depends on one single parameter, τ. Therefore, if we use the dimensionless time $\tilde{t} = t'/\tau$ Eq. (7) has a universal solution, i.e., the evolution of the reaction, as a function of dimensionless time does not depend on the heating rate:

$$\alpha(\tilde{t}) = 1 - exp\,[-exp\,(\tilde{t})]. \quad (8)$$

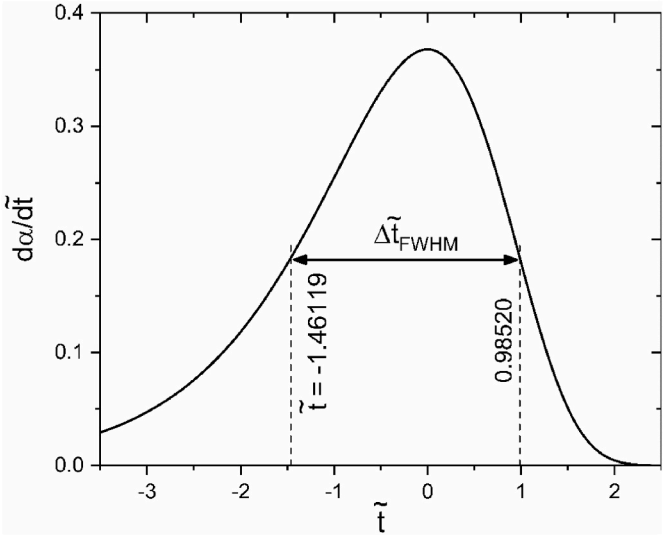

Fig. 5. Solid line: calculated evolution of the transformation rate vs. the dimensionless time according to Eq. (7). Dashed lines: dimensionless time at which the transformation rate is half the maximum transformation rate (full width at half maximum FWHM).

In Fig. 5 we have plotted the evolution of the transformation rate as a function of dimensionless time. To define $T_{o,r}$ we have taken half the maximum transformation rate. Thus, $T_{o,r}$ is given by $\tilde{t} = -1.46119$. Using the definition of dimensionless time and substituting it in Eq. (4) we obtain the following $T_{o,r}$:

$$T_{o,r} = T_{max}\left(1 - 1.46119\frac{R_G T_{max}}{E_A}\right). \quad (9)$$

In Fig. 6 we have plotted T_{max} and $T_{o,r}$ as a function of the heating rate for the kinetic parameters, A and E_A, given in Table 1. T_{max} and $T_{o,r}$ increase with heating rate. Therefore, to avoid overheating during the heating stage it is sufficient to select a heating rate high enough so that $T_{o,r}$ is above the temperature of the isothermal stage. Thus, from Eq. (9) we can determine a lower bound for β that avoids overheating during the constant heating rate stage. Nevertheless, as we will see in Section 5, the use of high heating rates to avoid a thermal runaway can have detrimental effects, such as inhomogeneous curing, due to the thermal inertia of the laminate.

On the other hand, the critical thickness depends on the heating rate (Sánchez-Rodriguez et al., 2017b), below a critical value the system reaches a quasi-stationary solution where heat generation is compensated by heat dissipation. So there is an upper limit for β below which there is no thermal runaway. According to ref (Sánchez-Rodriguez et al., 2017b). for a large surface area and assuming perfect thermal contact at the bottom and perfect thermal insulation at the top, the critical thickness is:

$$H_{c,0} = \frac{e^{1/\varepsilon}}{A}\sqrt{5\frac{\kappa\beta}{\rho q}\frac{0.878}{(1+2\varepsilon)\left\{1-(2+\varepsilon+30\varepsilon^2)\frac{2}{\theta_T}\right\}}}, \quad (10)$$

where $\varepsilon = \frac{R_G T_{max}}{E_A}$ and $\theta_T = \frac{E_A}{R_G T_{max}^2}\frac{q}{c}$.

The condition of perfect thermal insulation, however, is not realistic for manufacturing processes like vacuum infusion or hot plate pressing. Therefore, it is mandatory to adapt the condition developed in ref (Sánchez-Rodriguez et al., 2017b) to take into account the heat transport

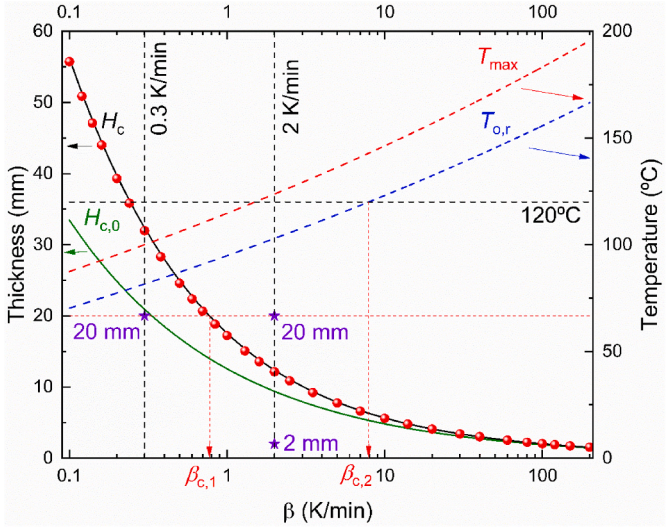

Fig. 6. Solid black and green lines: analytical prediction of the critical thickness assuming a convective coefficient of 70 W/m2K (Eq. (12)) or perfect insulation at the top (Eq. (10)), respectively. Symbols: numerical determination of the critical thickness assuming a convective coefficient of 70 W/m^{2}K. Red and blue dashed lines: calculated Kissinger and onset temperatures of the reaction according to Eqs. (6) and (9). The physical parameters used in the analytical and numerical results are given in Table 1. Purple stars: heating rate and thickness values corresponding to the two experiments and the results on the same composite laminate but of 2 mm thickness retrieved from [33].

by thermal convection at the top of the laminate as well as perfect thermal contact. For this purpose, we have reduced the numerical model Eqs. (1)–(3) to a one-dimensional model and integrated this model for the three sets of parameters indicated in Table 2: set 1 corresponds to a curing reaction (Esposito et al., 2016), and sets 2 and 3 to the decomposition of two different metalorganic precursors (Sánchez-Rodríguez et al., 2014; Zghal et al., 2020). In Table 2 we have considered significantly different systems to check the robustness of the model. For the numerical simulations, we have taken various heating rates from 5 to 30 K/min and different values of the convective coefficient between 0.001 and 5×10^8 W/m^{2}K. The result, Fig. 7, demonstrates that the relationship between the critical thickness and $H_{c,0}$ depends mainly on a single parameter which is the Biot number:

$$Bi_0 = h\frac{H_{c,0}}{\kappa}. \tag{11}$$

Note that when $h \to 0$, we obtain the expected solution for perfect insulation at the top, $H_c = H_{c,0}$.

Conversely, due to symmetry, a laminate of thickness $2H$ and perfect thermal contact at the top is equivalent to a laminate of thickness H and perfect thermal insulation at the top (Sánchez-Rodriguez et al., 2017a), so when $h \to \infty$ then $H_c \to 2H_{c,0}$. Thus, the critical laminate thickness changes by a factor of 2 when moving from perfect insulation to perfect thermal contact.

To quantify the dependence on the convective coefficient we fitted the numerical data in Fig. 6, and we obtained the following dependence:

$$H_c = H_{c,0}\left[2 - \left(1 + 0.63\left[h\frac{H_{c,0}}{k}\right]^{1.2}\right)^{-1}\right] \tag{12}$$

In Fig. 6 we have plotted the critical thickness as a function of the heating rate for the parameters given in Table 1 and $h = 70$ W/m^{2}K. We can observe that the higher the heating rate, the lower the critical thickness, thus, for a given thickness it is possible to obtain a lower limit for β so that for slower heating rate no thermal runaway will occur.

To confirm the validity of Eq. (12) we numerically integrated the partial differential equation and determined the critical thickness for heat rates ranging from 0.1 to 200 K/min. We integrated Eqs. (1)–(3) assuming a one-dimensional propagation of heat through the z direction and a perfectly thermalized mould. The parameters for the numerical integration are those in Table 1 with $h = 70$ W/m^{2}K. The result is shown in Fig. 6, and there is a perfect agreement between the numerical solution and the analytical one, Eq. (12).

Once Fig. 6 is generated, it can now be used to identify the two boundary cases that define three distinct scenarios. First, there is the lower boundary, $\beta_{c,1}$, the heating rate below which thermal runaway does not occur. This rate depends on the laminate thickness and can be identified by drawing a horizontal line from the left vertical axis to intersect with the H_c curve:

Table 2
Parameters for the numerical analysis of Fig. 7.

Property	Set 1 (Esposito et al., 2016)	Set 2 (Sánchez-Rodríguez et al., 2014)	Set 3 (Zghal et al., 2020)
Thermal conductivity, κ (W m^{-1} K^{-1})	0.54	0.06	0.0846
Specific heat capacity, c (J kg^{-1} K^{-1})	975	875	1010
Density, ρ (kg m^{-3})	1525	1114	578
Specific heat of reaction, q (J kg^{-1})	2.5×10^5	2.75×10^5	3.74×10^6
Activation energy, E_A (J mol^{-1})	7.985×10^4	1.70×10^5	2.20×10^5
Pre-exponential constant, A (s^{-1})	1.08×10^9	3.4×10^{13}	2.34×10^{19}

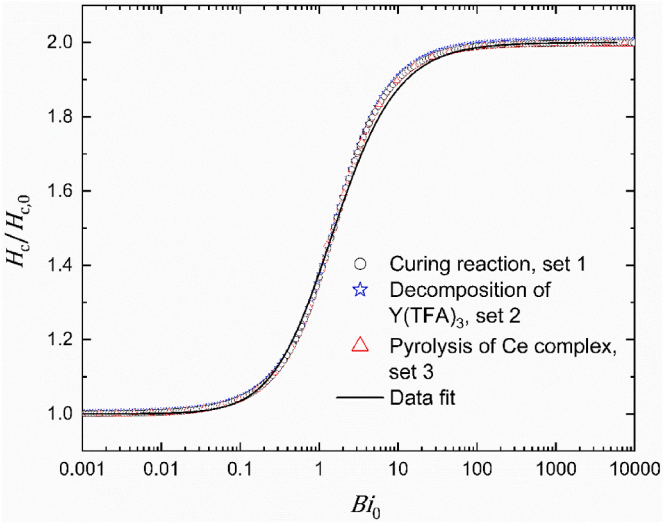

Fig. 7. Symbols: numerical analysis of the ratio between the critical thickness, H_c, and the theoretical critical thickness for perfect insulation at the top, Eq. (10), as a function of the Biot number, Eq. (11). The analysis was carried out for the three sets of parameters given in Table 2. Solid line data fit, Eq. (12).

$\beta > \beta_{c,1} \rightarrow$ *Homogeneous curing*

Secondly, there is the upper boundary, $\beta_{c,2}$, beyond which thermal runaway is also avoided, as the temperature at which thermal runaway would occur exceeds the isothermal stage temperature of a curing cycle composed of a ramp followed by a dwell period. However, as previously noted, this condition promotes high thermal gradients that lead to uneven curing. This limit is defined by drawing a horizontal line from the right vertical axis at the dwell temperature to intersect the $T_{o,r}$ curve:

$\beta > \beta_{c,2} \rightarrow$ *Unhomogeneous curing*

The third scenario occurs when the heating rate during the ramp stage falls between $\beta_{c,1}$ and $\beta_{c,2}$, defining the heating ramp range where thermal runaway is expected:

$\beta_{c,1} < \beta < \beta_{c,2} \rightarrow$ *Thermal runaway*

5. Experimental validation

The manufacturer's recommended cure cycle (MRCC) for the VTC401 epoxy resin consists of a ramp up to 120 °C at 2 °C/min, a dwell at 120 °C for 45 min, a second ramp to 135 °C at 0.3 °C/min, a second dwell at 135 °C for 2 h and then cooling to room temperature at 2 °C/min (Fig. 7). The temperature evolution along a 20-mm-thick CFRP laminate with VTC401 epoxy resin laminate was experimentally determined using embedded thermocouples during MRCC (Fig. 1). In Fig. 8 we have plotted the temperature evolution of the thermocouple that recorded the maximum and minimum temperature, thermocouple TC3 and TC2, respectively. Fig. 8 clearly shows an overshoot at the end of the heating stage, despite the fact that the thermal program strictly conforms to the manufacturer's data sheet.

In Fig. 9 we have plotted the temperature evolution recorded by all the embedded thermocouples, together with the temperature evolution at different locations (Fig. 4) obtained from the numerical integration of Eqs. (1)–(3) for a 20-mm-thick panel. For the numerical simulation, we have taken the physical parameters of the M55J/VTC401 unidirectional carbon epoxy prepreg (Table 1), and a convective coefficient of 70 W/m^{2}K (Esposito et al., 2016; Guo et al., 2005). We have also considered that the bottom the panel is in contact with a 15-mm-thick aluminium mould ($\kappa = 117$ W/mK, $c = 900$ J/kgK and $\rho = 2660$ kg/m^3 (Esposito et al., 2016)).

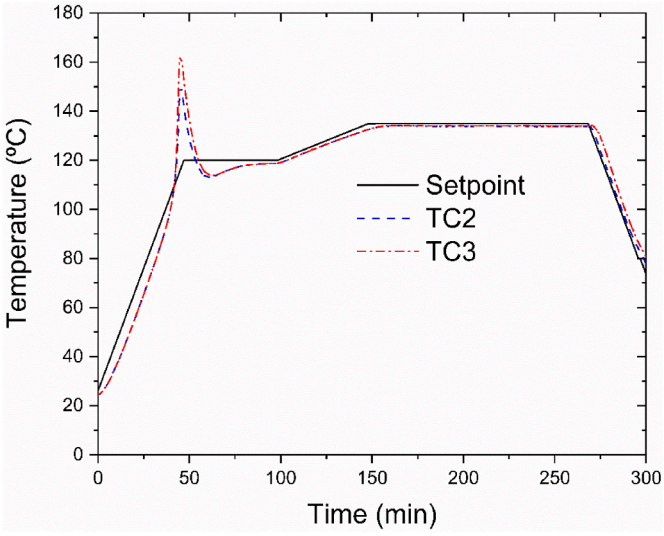

Fig. 8. Black solid line: manufacturer's recommended cure cycle (MRCC) for the VTC401 epoxy resin. Blue dashed and red dot-dashed lines: evolution of temperatures recorded by thermocouple TC3 and TC2 in a 20-mm-thick panel (Fig. 1).

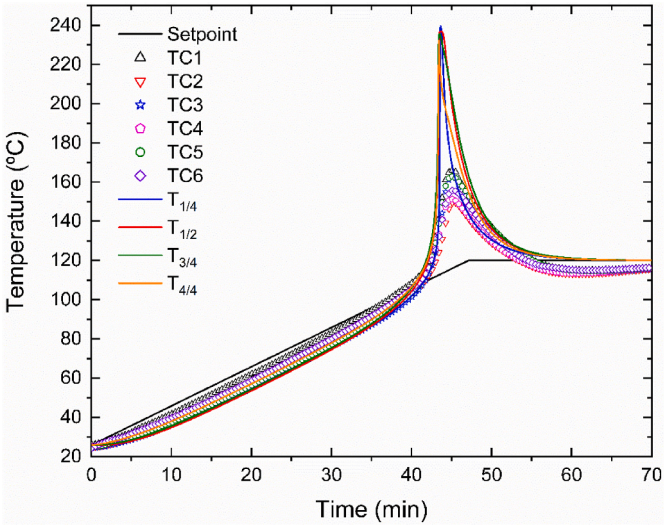

Fig. 9. Symbols: Experimental evolution of temperature recorded by the thermocouples embedded across the thickness of the panel (Fig. 1). Continuous lines: calculated temperature evolution predicted by numerical integration, Eqs. (1)–(3), for a 20-mm-thick laminate at positions located at 5 (1/4), 10 (1/2), 15 (3/4) and 20 mm (4/4) away from the mould (see Fig. 4 for details).

The numerical simulation reproduces the initial phases of thermal overshoot fairly well; however, the subsequent evolution shows higher temperature values for the simulation. The reason is that the autoclave has a self-regulating system based on the sample temperature which is designed to avoid temperature overshoot. Thus, when the temperature of the laminate starts to deviate from the setpoint, the autoclave cools down. This self-regulating control also explains that once the overshoot has passed, time >60 min, the numerical simulation recovers the setpoint temperature while the temperature recorded on the panel is clearly below the setpoint, i.e., the mould temperature is lower than the setpoint temperature.

To avoid a thermal overshoot for a 20 mm thick laminate, according to the analytical model we selected a slower heating ramp. For this purpose, from Fig. 6, we chose a heating rate close to the critical condition for perfect insulation, 0.3 K/min. We have repeated the curing cycle for a 20 mm thick laminate, but replacing the initial heating ramp of 2 K/min by a heating ramp of 0.3 K/min. The temperature evolution during this curing cycle is shown in Fig. 10. Unfortunately, for an unknown reason at the initial stage the autoclave did not follow the programmed setpoint and, after 200 min, the autoclave exceeded the programmed rate to catch up. As we have seen in Figs. 8 and 9, the thermal overshoot appears at the end of the heating ramp, as it approaches the temperature of 120 °C. Fortunately, the heating ramp reached again the programmed rate of 0.3 K/min before the end of this first stage, so the autoclave followed the heating rate programmed in the critical stage. From Fig. 10, we can confirm that there is perfect thermalization throughout the sample and no thermal gradients are observed, as predicted by our analytical model.

5.1. *The effect of curing overheating on the T_g*

Differences in T_g of 5.5 °C (5.1 %) appeared between the specimens extracted from the tool-ply interface and the mid-inside zone of the thick laminate submitted to the MRCC (Fig. 3), experimentally confirming that the cure process across the 20-mm-thick panel was not uniform. Furthermore, the T_g for the mid-inner specimen is 10.4 °C lower than the T_g determined in a non-overheated thin panel (2 mm) following the MRCC (González et al., 2024), which in turn means that in the worst-case scenario, the overheated samples extracted from the thick panel exhibit a maximum T_g drop of 9.3 % related to the thermal degradation (Fig. 11).

6. Discussion

Both the experimental data and the numerical simulation show that, in the case of a thick laminate and for the MRCC, the reaction becomes unstable, and a thermal runaway occurs, resulting in a sharp overheating (Figs. 8 and 9). When a thermal runaway takes place, the heat generated by the curing process in the central area of the panel cannot be dissipated efficiently and the curing reaction is further accelerated. This local overheating may be detrimental for the final properties and must be avoided during composites processing (Twardowski et al., 1993).

In Fig. 6 we have represented the two experimental cases performed on the same composite laminate: a 2-mm-thick panel (González et al., 2024) and a 20-mm-thick panel (Fig. 8). In both cases, the temperature program is the MRCC. In the case of the 2-mm panel there is no

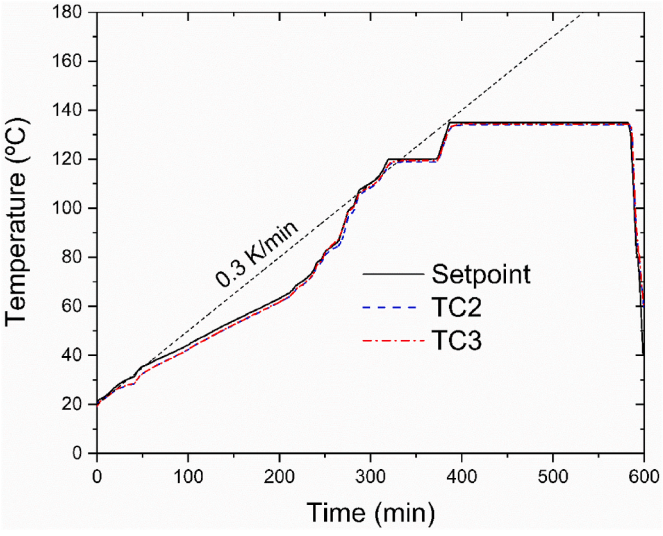

Fig. 10. Black solid line: autoclave temperature setpoint. Blue dashed and red dot-dashed lines: experimental evolution of temperatures recorded by thermocouples TC3 and TC2 in a 20-mm-thick panel (Fig. 1). Black dashed line: programed initial heating ramp.

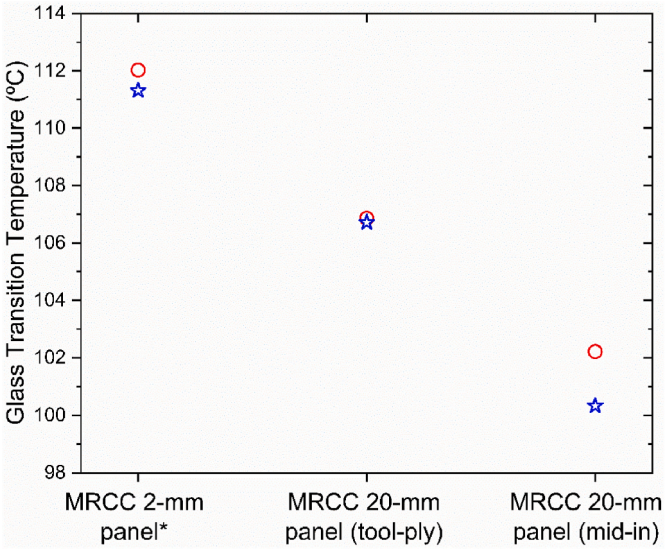

Fig. 11. Experimental measurement of the glass transition temperature after applying the MRCC for a 2- and 20-mm-thick laminate. Two samples, red circles and blue stars, were analysed for each case. *T_g for MRCC 2 mm-thick panel retrieved from (González et al., 2024).

overheating and the thermal gradients are negligible during the complete curing cycle (Fig. 4 in (González et al., 2024)), while for the 20-mm-thick panel overheating occurs during the heating stage at 2 K/min. From Fig. 6 we can confirm that the critical thickness for $\beta = 2$ K/min, obtained from Eq. (12), 12.4 mm, lies between 2 and 20 mm, thus in agreement with the experimental result.

However, as we have seen in Section 4, two conditions must be fulfilled for a thermal runaway to occur during the constant heating stage: (i) the panel thickness must be greater than the critical thickness, and (ii) the final temperature of the heating stage must be greater than the onset temperature, Eq. (9). We have already determined that the first condition is only satisfied in the case of the 20-mm-thick laminate. As for the second condition, we have plotted the final temperature of the heating stage, 120 °C, as a horizontal line in Fig. 6. It can be seen that the onset temperature for $\beta = 2$ K/min is below this horizontal line, so the second condition is also fulfilled. However, this horizontal line is slightly below the Kissinger temperature. Consequently, overheating occurs at the end of the heating phase, as seen in Figs. 9 and 10.

According to the analytical model, there are two possible strategies to avoid thermal runaway. The first one is to reduce the heating rate so that the critical thickness is greater than 20 mm. This critical heating rate can be determined from Fig. 6. Indeed, we have drawn a horizontal line corresponding to the 20-mm thickness, and from the intersection with the critical thickness curve we determined that for a heating rate of 0.3 K/min no thermal runaway is expected to occur in 20 mm thick panels, even under perfect insulation conditions. We have subjected a 20-mm thick panel to a curing cycle with an initial heating ramp of 0.3 K/min and no thermal gradients were observed, confirming that the occurrence of thermal runaway has been avoided, as seen in Fig. 10.

The second strategy to prevent runaway is to choose a heating rate high enough so that the onset temperature is above the temperature of the isothermal stage. Again, this lower limit of the heating rate can be determined with the help of Fig. 6. In this case, from the intersection between the onset temperature curve and the horizontal line corresponding to the isothermal temperature, i.e., 120 °C. This intersection gives the limiting heating rate as 7.91 K/min. That is, for heating rates higher than this value, no thermal runaway occurs during the heating stage below 120 °C.

Nevertheless, this second strategy has a handicap. When the panel is heated at a high heating rate, thermal gradients are formed due to the thermal inertia of the panel. In the Appendix we have determined the time lag related to the thermal inertia of the panel, τ_{lag}:

$$\tau_{lag} = \frac{1}{a}\left(B\frac{H}{\pi}\right)^2, \tag{13}$$

where $a = \frac{\kappa}{\rho c}$ is the thermal diffusivity and B is a constant that depends on the convective coefficient, given by Eq. (A.10) and ranging from 1 when $h = \infty$ to 2 when $h = 0$. In Fig. 12 we have plotted the evolution of this time lag as a function of the laminate thickness for $h = 0$, $h = 70$ W/m^{2}K and $h = \infty$. Note that this time lag scales as the square of the thickness.

According to the Appendix, when a sample is heated at a constant heating rate, this time lag results in a maximum temperature difference within the sample of:

$$\Delta T = 1.2331\beta\tau \tag{14}$$

In our case, for a thickness of 20 mm and $h = 70$ W/m^{2}K, we obtain $\tau = 187$ s. Thus, for a heating rate of 2 K/min we obtain a maximum temperature difference of 7.7 °C which is in agreement with the maximum temperature difference recorded within the panel (Fig. 9 between thermocouples TC1 and TC3) during the first heating stage and before reaching the region affected by the heat released by the curing reaction (<35 min).

Besides, for a heating rate of 7.91 K/min we obtain $\Delta T = 30$ °C, i.e., using a high heating ramp to avoid thermal runaway leads to temperature differences inside the sample of more than 30 °C. This fact discourages using the second strategy mentioned above in the manufacturing of composites in industrial contexts.

7. Conclusions

In the case of thick panels, a thermal overshoot may occur in the first heating ramp during manufacturing, even if the curing cycle strictly complies with the manufacturer's recommendations.

We have analytically determined the conditions that should be met to avoid a thermal overshot during the heating stage. Indeed, three different approaches are available. First, we have shown that there is a threshold heating rate below which no thermal runaway occurs. Although this strategy involves a longer curing cycle it ensures that no significant temperature differences within the sample will arise.

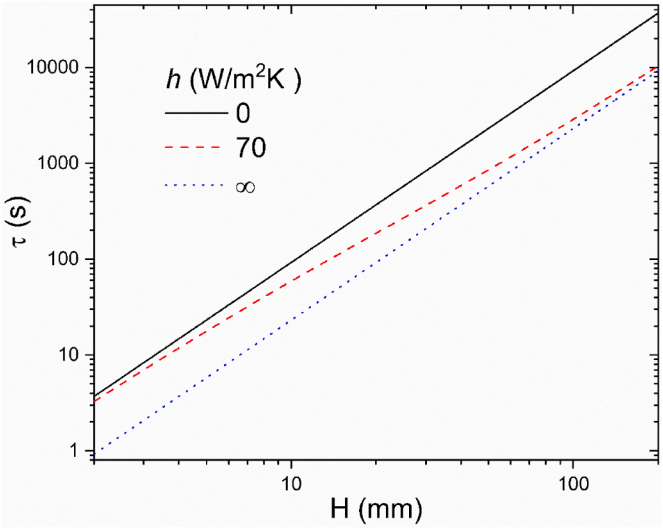

Fig. 12. Calculated time lag, Eq. (14) as a function of the panel thickness for the physical parameters of Table 1 and three different boundary conditions on top: perfect insulation ($h = 0$), convection with $h = 70$ W/m^{2}K, and perfect thermal contact $h = \infty$.

Conversely, a thermal overshoot can also be avoided by choosing a heating rate higher than a critical heating rate. However, in this case significant temperature differences arise within the sample due to the thermal inertia of the panel.

As a third option, the occurrence of a thermal runaway can be prevented by limiting the laminate thickness to below the critical one.

The analytical prediction of these two limiting heating rates, as well as the analytical determination of the temperature differences within the sample due to thermal inertia, have been validated against a numerical analysis. The agreement between the analytical solution and the numerical analysis is remarkable.

Finally, we have experimentally processed two 20-mm-thick panels instrumented with thermocouples across the thickness. One of the panels has been processed according to the MRCC while the second one has been processed according to a modified curing cycle with a limited heating rate determined through an analytical prediction. It has been observed that thermal runaway occurs for the MRCC while it is avoided with the modified curing cycle. Moreover, it has also been shown that numerical simulation and analytical predictions reproduce the experimental results.

CRediT authorship contribution statement

Jordi Farjas: Writing – original draft, Supervision, Methodology, Conceptualization. **José Antonio González:** Investigation, Formal analysis. **Daniel Sánchez-Rodríguez:** Writing – review & editing. **Norbert Blanco:** Writing – review & editing, Supervision. **Marc Gascons:** Supervision, Resources, Project administration. **Josep Costa:** Writing – review & editing, Supervision, Resources, Project administration.

Declaration of competing interest

The authors declare that they have no known competing financial interests or personal relationships that could have appeared to influence the work reported in this paper.

Acknowledgements

This study was supported by the *Generalitat de Catalunya* [Industrial Doctorate grant, contract no. 2018DI0053]; the Ministry of Research and Universities of the Government of Catalonia [Beatriu de Pinós Programme, fellowship BP00069]; and the Spanish *Agencia Estatal de Investigación* [project PID 2021-126989OB-I00/10.13039/501100011033/FEDER, UE].

Appendix. Thermal inertia

In this appendix, we determine the characteristic time constant related to the thermal inertia in order to estimate the maximum temperature variations that appear when the panel is heated at a constant heating rate. To do so, we will use a simplified one-dimensional model without substrate:

$$\rho c\frac{\partial T}{\partial t}=\kappa\frac{\partial^2 T}{\partial z^2}, \tag{A.1}$$

with the boundary conditions:

$$T(0)=T_m, \kappa\left.\frac{\partial T}{\partial z}\right|_{z=H}=h[T_m-T(H)]. \tag{A.2}$$

We solve this PDE system through separation of variables:

$$T(y,t)=T_m+f(t)g(z), \tag{A.3}$$

substituting Eq. (A.3) into Eq. (A.1) gives the following equation:

$$\frac{1}{af(t)}\frac{df(t)}{dt}=\frac{1}{g(z)}\frac{d^2g(z)}{dz^2}, \tag{A.4}$$

where $a=\frac{\kappa}{\rho c}$ is the thermal diffusivity.

Eq. (A.4) must be satisfied for all z and all t, but the left side does not depend on z and the right side does not depend on t. Thus, each side must be a constant. We call this $-\gamma^2$ for convenience.

Thus, for the function $f(t)$ we obtain the following differential equation:

$$\frac{df(t)}{f(t)}=-a\gamma^2 dt\rightarrow f(t)=f(0)e^{-t/\tau_{lag}}, \tag{A.5}$$

where $\tau_{lag}=\frac{1}{a\gamma^2}$ is the characteristic time scale for thermalization. To determine the value of γ we need to solve the differential equation for $g(z)$:

$$\frac{d^2g(y)}{dz^2}=-\gamma^2 g(z). \tag{A.6}$$

The solution of Eq. (A.5) is a sinusoidal function, for instance:

$$g(z)=\sin(\gamma z+\psi), \tag{A.7}$$

where ψ and γ depend on the boundary conditions, Eq. (A.2). Since $T(0)=T_m$ then $g(0)=0$. Besides, due to the thermal inertia the temperature decreases when y increases thus $\psi=\pi$:

$$g(z)=-\sin(\gamma z). \tag{A.8}$$

Then substituting Eq. (A.3) and **(A.8)**, into the second boundary condition, Eq. (A.2) gives:

$$\gamma \cos(\gamma H) = -\frac{h}{\kappa}\sin(\gamma H). \tag{A.9}$$

Since the Biot number is defined as $Bi = h\frac{H}{\kappa}$, from Eq. (A.9) the determination of γ is reduced to solve the following equation:

$$Bi = -\frac{\gamma H}{\tan(\gamma H)} \tag{A.10}$$

For example, if we assume $h = 0$, then $Bi = 0$, $\gamma = \frac{\pi}{2H}$ and $\tau_{lag} = \frac{1}{a}\left(\frac{2H}{\pi}\right)^2$. Also, if we assume $h = \infty$, then $Bi = \infty$, $\gamma = \frac{\pi}{H}$, and $\tau_{lag} = \frac{1}{a}\left(\frac{H}{\pi}\right)^2$. This factor of 2 between the two limiting cases is expected since, as mentioned in Section 4, the case of perfect thermal contact is equivalent to perfect insulation of thickness $2H$.

Due to this time lag, when a panel is heated at a constant rate β, a temperature distribution appears within the sample, and the maximum temperature difference with respect to the mould is proportional to:

$$\Delta T = C\beta\tau_{lag} \tag{A.11}$$

where C is a dimensionless constant. To determine this constant, we have numerically determined ΔT with respect to $\beta\tau_{lag}$ for three different heating rates, for $h = 0$ and for the physical parameters in Table 1. The result is shown in Fi gure A.1 and, as predicted by Eq. (A.11), we obtain a perfect linear fit passing through the origin of coordinates. From this linear fit we have determined that $C = 1.2331$.

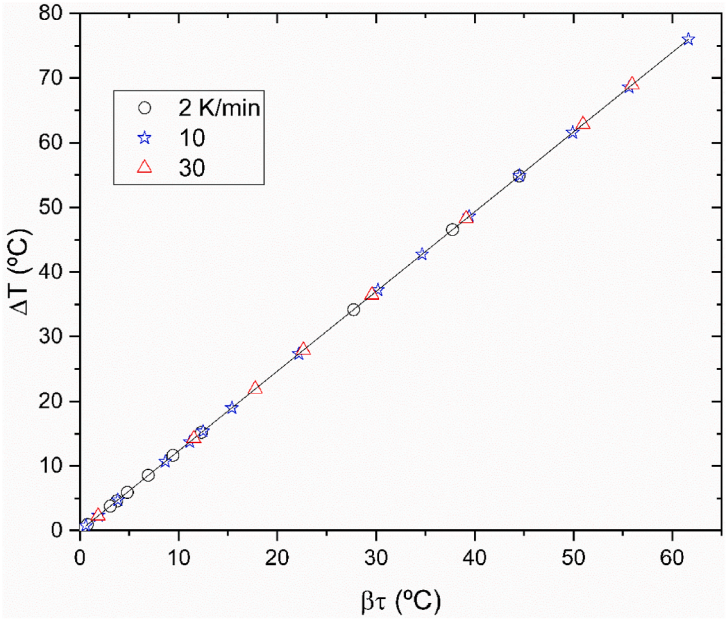

Fig. A.1. Symbols: Calculated maximum temperature difference within a panel determined from the numerical integration of Eq. (A.1) and (A.2). The physical parameters correspond to Table 1 with h = 0. The different values have been obtained by varying the panel thickness from 2 to 38 mm and for three different heating rates. Solid line: linear fit.

Finally, to check the dependence of τ on the Biot number, we have numerically calculated ΔT with respect to Bi for the physical parameters in Table 1 with $\beta = 10$ K/min, $H = 5$ mm and h varying from 0.01 to 10^6 W/m^{2}K and compared it with the theoretical result obtained from Eq. (A.11) with $C = 1.2331$ and γ determined from Eq. (A.10). The result is shown in Fi gure A.2 and confirms that there is a perfect agreement between the theoretical prediction and the numerical solution.

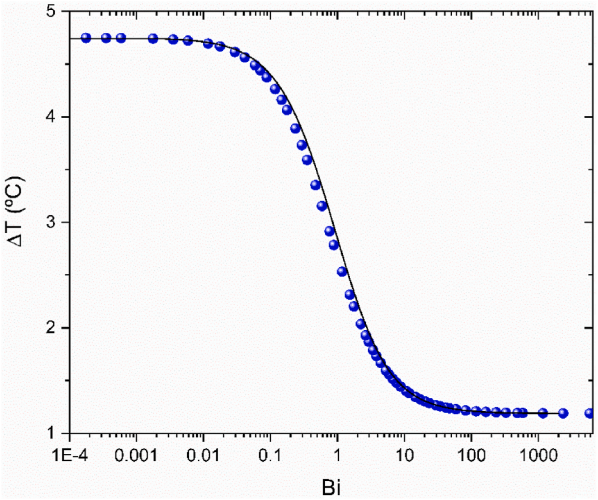

Fig. A.2. Symbols: Calculated maximum temperature difference within a panel determined from the numerical integration of Eq. (A.1) and (A.2). The physical parameters correspond to Table 1 with $\beta = 10$ K/min, $H = 5$ mm and h varying from 0.01 to 106 W/m2K. Solid line: analytical prediction from Eq. (A.10) and (A.11) with $C = 1.2331$.

Data availability

Data will be made available on request.

References

Adler, J., Enig, J.W., 1964. The critical conditions in thermal explosion theory with reactant consumption. Combust. Flame 8 (2), 97–103. https://doi.org/10.1016/0010-2180(64)90035-5.

Antonucci, V., Giordano, M., Inserraimparato, S., Nicolais, L., 2001. Analysis of heat transfer in autoclave technology. Polym. Compos. 22 (5), 613–620. https://doi.org/10.1002/pc.10564.

Barzykin, V.V., 1973. Thermal explosion under linear heating. Combust. Explos. Shock Waves 9 (1), 29–42. https://doi.org/10.1007/BF00740358.

Bogetti, T.A., Gillespie, J.W., 1991. Two-dimensional cure simulation of thick thermosetting composites. J. Compos. Mater. 25 (3), 239–273. https://doi.org/10.1177/002199839102500302.

Budrugeac, P., Segal, E., 2007. Applicability of the kissinger equation in thermal analysis revisited. Journal of Thermal Analysis and Calorimetry; 9th European Symposium on Thermal Analysis and Calorimetry 88 (3), 703–707. https://doi.org/10.1007/s10973-006-8087-z.

Ciriscioli, P.R., Wang, Qiuling, Springer, G.S., 1992. Autoclave curing — comparisons of model and test results. J. Compos. Mater. 26 (1), 90–102. https://doi.org/10.1177/002199839202600106.

Criado, J.M., Ortega, A., 1986. Non-isothermal transformation kinetics: remarks on the Kissinger method. J. Non-Cryst. Solids 87 (3), 302–311. https://doi.org/10.1016/S0022-3093(86)80004-7.

Dolkun, D., Zhu, W., Xu, Q., Ke, Y., 2018. Optimization of cure profile for thick composite parts based on finite element analysis and genetic algorithm. J. Compos. Mater. 52 (28), 3885–3894. https://doi.org/10.1177/0021998318771458.

Esposito, L., Sorrentino, L., Penta, F., Bellini, C., 2016. Effect of curing overheating on interlaminar shear strength and its modelling in thick FRP laminates. Int. J. Adv. Des. Manuf. Technol. 87 (5–8), 2213–2220. https://doi.org/10.1007/s00170-016-8613-5.

Farjas, J., Butchosa, N., Roura, P., 2010. A simple kinetic method for the determination of the reaction model from non-isothermal experiments. J. Therm. Anal. Calorim. 102 (2), 615–625. https://doi.org/10.1007/s10973-010-0737-5.

Farjas, J., Camps, J., Roura, P., Ricart, S., Puig, T., Obradors, X., 2012. The thermal decomposition of barium trifluoroacetate. Thermochim. Acta 544 (0), 77–83. https://doi.org/10.1016/j.tca.2012.06.020.

Farjas, J., Roura, P., 2008. Simple approximate analytical solution for nonisothermal single-step transformations: kinetic analysis. AIChE J. 54 (8), 2145–2154. https://doi.org/10.1002/aic.11540.

Farjas, J., Roura, P., 2014. Exact analytical solution for the Kissinger equation: determination of the peak temperature and general properties of thermally activated transformations. Thermochim. Acta 598, 51–58. https://doi.org/10.1016/j.tca.2014.10.024.

Gao, Y., Lin, Z., Zhou, Y., Ling, Z., Dong, J., Wang, H., Peng, H.X., 2023. Size effect in curing optimization for thick composite laminates. Mater. Today Commun. 34 (December 2022), 105276. https://doi.org/10.1016/j.mtcomm.2022.105276.

González Ruiz, J.A., Farjas, J., Blanco, N., Costa, J., Gascons, M., 2022. Assessment of unexplored isoconversional methods to predict epoxy-based composite curing under arbitrary thermal histories. J. Reinforc. Plast. Compos. https://doi.org/10.1177/07316844221145591, 073168442211455.

González, Jose, Farjas, Jordi, Blanco, Norbert, Costa, Josep, Gascons Tarres, Marc, Sánchez, D., 2024. Towards time-reduced cure cycles for mass production of composites maintaining the thermo-mechanical properties. Journal of Thermal Analysis and Calorimetry. https://doi.org/10.1007/s10973-024-13442-8.

Guo, Z.S., Du, S., Zhang, B., 2005. Temperature field of thick thermoset composite laminates during cure process. Compos. Sci. Technol. 65 (3–4), 517–523. https://doi.org/10.1016/j.compscitech.2004.07.015.

Kissinger, H.E., 1957. Reaction kinetics in differential thermal analysis. Anal. Chem. 29 (11), 1702–1706. https://doi.org/10.1021/ac60131a045.

Lorenz, N., Müller-Pabel, M., Gerritzen, J., Müller, J., Gröger, B., Schneider, D., Fischer, K., Gude, M., Hopmann, C., 2022. Characterization and modeling cure- and pressure-dependent thermo-mechanical and shrinkage behavior of fast curing epoxy resins. Polym. Test. 108. https://doi.org/10.1016/j.polymertesting.2022.107498.

Ltd SCM, 2018. VTC401 Epoxy Component Prepreg. Product Data.

Merzhanov, A.G., Strunina, A.G., 1965. Laws of thermal explosion with constant heating rate. Combust. Explos. Shock Waves 1 (1), 43–52. https://doi.org/10.1007/BF00757151.

Michaud, D.J., Beris, A.N., Dhurjati, P.S., 2002. Thick-sectioned RTM composite manufacturing: Part I – in situ cure model parameter identification and sensing. J. Compos. Mater. 36 (10), 1175–1200. https://doi.org/10.1177/0021998302036010589.

Oh, J.H., Lee, D.G., 2002. Cure cycle for thick glass/epoxy composite laminates. J. Compos. Mater. 36 (1), 19–45. https://doi.org/10.1177/0021998302036001300.

Press, W.H., Flannery, B.P., Teukolsky, S.A., Vetterling, W.T., 1994. Numerical Recipes in C: the Art of Scientific Computing, 2nd. Cambridge University Press.

Roura, P., Farjas, J., 2009. Analytical solution for the Kissinger equation. J. Mater. Res. 24 (10), 3095–3098. https://doi.org/10.1557/jmr.2009.0366.

Sánchez-Rodríguez, D., Eloussifi, H., Farjas, J., Roura, P., Dammak, M., 2014. Thermal gradients in thermal analysis experiments: criterions to prevent inaccuracies when determining sample temperature and kinetic parameters. Thermochim. Acta 589, 37–46. https://doi.org/10.1016/j.tca.2014.05.001.

Sánchez-Rodríguez, D., Farjas, J., Roura, P., 2017a. The critical condition for thermal explosion in an isoperibolic system. AIChE J. 63 (9), 3979–3993. https://doi.org/10.1002/aic.

Sánchez-Rodríguez, D., Farjas, J., Roura, P., 2017b. The critical conditions for thermal explosion in a system heated at a constant rate. Combust. Flame 186, 211–219. https://doi.org/10.1016/j.combustflame.2017.08.008.

Sánchez-Rodríguez, D., Wada, H., Yamaguchi, S., Farjas, J., Yahiro, H., 2017. Synthesis of LaFeO3 perovskite-type oxide via solid-state combustion of a cyano complex precursor: the effect of oxygen diffusion. Ceram. Int. 43 (3), 3156–3165. https://doi.org/10.1016/j.ceramint.2016.11.134.

Šesták, J., Holba, P., Živković, Ž., 2014. Doubts on kissinger's method of kinetic evaluation based on several conceptual models showing the difference between the maximum of reaction rate and the extreme of a dta peak. J. Min. Metall. B Metall. 50 (1), 77–81. https://doi.org/10.2298/JMMB130902006S.

Shi, L., 2016. Heat transfer in the thick thermoset composites [TUDelft]. In: Masters Thesis - Northwestern Polytechnical University. https://doi.org/10.4233/uuid:9e8e9c3a-edc3-49a0-ae6b-980bb2eea5e5.

Sorrentino, L., Esposito, L., Bellini, C., 2017. A new methodology to evaluate the influence of curing overheating on the mechanical properties of thick FRP laminates. Compos. B Eng. 109, 187–196. https://doi.org/10.1016/j.compositesb.2016.10.064.

Tifkitsis, K.I., Mesogitis, T.S., Struzziero, G., Skordos, A.A., 2018. Stochastic multi-objective optimisation of the cure process of thick laminates. Compos. Appl. Sci. Manuf. 112 (June), 383–394. https://doi.org/10.1016/j.compositesa.2018.06.015.

Tranchard, P., Samyn, F., Duquesne, S., Estèbe, B., Bourbigot, S., 2017. Modelling behaviour of a carbon epoxy composite exposed to fire: Part I—characterisation of thermophysical properties. Materials 10 (5), 494. https://doi.org/10.3390/ma10050494.

Twardowski, T.E., Lin, S.E., Geil, P.H., 1993. Curing in thick composite laminates: experiment and simulation. J. Compos. Mater. 27 (3), 216–250. https://doi.org/10.1177/002199839302700301.

Varma, A., Morbidelli, M., Wu, H., 1999. Parametric Sensitivity in Chemical Systems. Cambridge University Press.

Victor, A.C., 1995. Simple calculation methods for munitions cookoff times and temperatures. Propellants, Explos. Pyrotech. 20 (5), 252–259. https://doi.org/10.1002/prep.19950200506.

Voto, G., Sequeira, L., Skordos, A.A., 2019. Heating rate limits in fast cure processing of thick carbon fibre laminates. ECCM 2018 - 18th European Conference on Composite Materials, pp. 24–28. June.

VTC401 Epoxy Component Prepreg, 2018. Product Data. SHD Composite Materials Ltd; February.

Zghal, I., Farjas, J., Camps, J., Sánchez-Rodríguez, D., Dammak, M., Roura-Grabulosa, P., 2020. Use of thermal analysis to predict the conditions for thermal explosion to occur: application to a Ce triethanolamine complex. J. Therm. Anal. Calorim. 142 (5), 2087–2094. https://doi.org/10.1007/s10973-020-10262-4.

Zhang, G., Luo, L., Lin, T., Zhang, B., Wang, H., Qu, Y., Meng, B., 2021. Multi-objective optimisation of curing cycle of thick aramid fibre/epoxy composite laminates. Polymers 13 (23), 4070. https://doi.org/10.3390/polym13234070.